A poxviral homolog of the Pellino protein inhibits Toll and Toll-like receptor signalling

Bryan D. Griffin[*1,2], *Mark Mellett*[*1], *Antonio Campos-Torres*[1], *Gemma K. Kinsella*[1], *Bingwei Wang*[1] and *Paul N. Moynagh*[1]

[1] Institute of Immunology, National University of Ireland, Maynooth, County Kildare, Ireland
[2] Department of Medical Microbiology, University Medical Centre Utrecht, Utrecht, The Netherlands

Toll-like receptor (TLR) signalling pathways constitute an evolutionarily conserved component of the host immune response to pathogenic infection. Here, we describe the ability of a virally encoded form of the Pellino protein to inhibit Toll- and TLR-mediated activation of downstream Rel family transcription factors. In addition to inhibiting *drosomycin* promoter activation by Spätzle in *Drosophila melanogaster* cells, viral Pellino attenuates the activation of NF-κB by TLR signalling components and by the TLR4 ligand, LPS, in human cells. We propose that viral Pellino, like mammalian Pellinos, contains a forkhead-associated domain but differs from the mammalian forms in that it lacks a complete and functional RING-like domain. We produce a homology model and present experimental data to support this model by demonstrating that, like mammalian Pellinos, viral Pellino can interact with IRAK-1 via its forkhead-associated domain, whereas unlike its mammalian counterparts, it fails to post-translationally modify IRAK-1. Furthermore, we demonstrate that viral Pellino can functionally antagonise the activity of human Pellino3S. Thus, our findings identify potential immunoevasive capabilities possessed by a poxviral homolog of the Pellino protein and add growing evidence for a likely role for Pellino proteins in Toll and TLR signalling.

Keywords: Innate immunity · Pellino · Signal transduction · Toll-like receptors

Introduction

Chief among innate immune signalling pathways is Toll-like receptor (TLR) signalling to NF-κB, which controls expression of regulatory molecules that co-ordinate humoral and cell-mediated immunity [1]. Many details of this axis were unravelled based on the evolutionary conservation with the parallel immune defence response in *Drosophila*, where the Spätzle/Toll/Pelle/Cactus axis regulates induction of antimicrobial peptides [2]. Upon ligand binding, all TLRs except TLR3 recruit the adaptor protein MyD88 and the kinases IRAK-1 and IRAK-4 [3]. TLR2 and -4 signalling require the adaptor Mal to bridge the receptor and MyD88 [4].

IRAK-4 phosphorylates IRAK-1, leading to IRAK-1 autophosphorylation [5]. The kinases then leave the receptor to interact with TRAF6. Next, TRAF6 promotes the generation of unanchored lysine 63 polyubiquitin chains [6], leading to activation of the downstream kinase TAK-1 [7, 8]. This in turn can lead to activation of MAPK signalling, as well as stimulation of IKK activity. IKKβ phosphorylates IκB proteins, leading to their ultimate degradation and the ensuing liberation of NF-κB [9].

An emerging aspect of control in TLR signalling is the role of Pellino proteins [10, 11]. Pellino was first identified in *Drosophila* as a binding partner of Pelle, a *Drosophila* homolog of IRAK [12]. Pellino acts as a positive regulator of innate immunity in *Drosophila* by promoting the induction of the antimicrobial peptide drosomycin [13]. Three members of the mammalian

Correspondence: Prof. Paul N. Moynagh
e-mail: Paul.Moynagh@nuim.ie

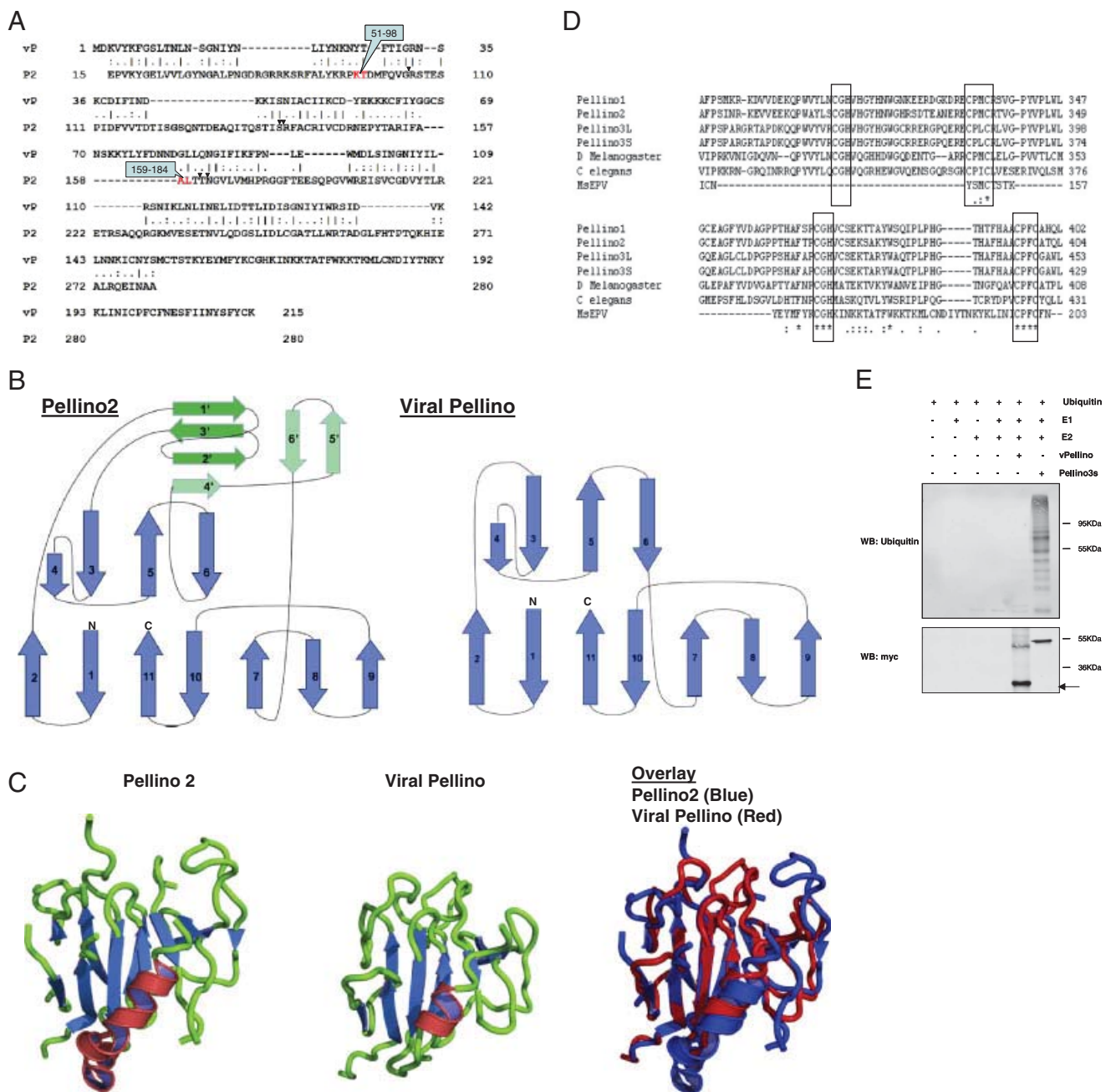*These authors have contributed equally to this work.

Figure 1. Homology modeling of viral Pellino. (A) Alignment between the viral Pellino amino acid sequence and the FHA domain sequence of the available Pellino2 crystal structure (PDB:3EGB). The black triangles indicate highly conserved residues in core FHA domains e.g. R106, S137, R138, T187 and N188 in Pellino2. The residues highlighted in red border the regions 51–98 and 159–184 of Pellino2 which have been omitted for space considerations. (B) Topology diagrams of Pellino2 and viral Pellino with β strands of core FHA domain in blue and of non-canonical wing in green. (C) FHA domain of the Pellino 2 (PDB:3EGB) crystal structure (left image); comparative model of viral Pellino modeled as an FHA domain (middle image), where the α helices are represented in red, β strands in blue and loop regions in green. Pellino 2 (PDB:3EGB) crystal structure in blue overlaid with the comparative model of viral Pellino modeled as an FHA domain (in red) (right image). Visualisation was performed with PyMOL (De Lano Scientific, USA). (D) ClustalW alignment of amino acid sequences from the C-terminal region of human Pellinos 1, 2, 3L and 3S, *Caenorhabditis elegans* Pellino, *Drosophila* Pellino and viral Pellino. The boxed residues form the RING domain. (E) Recombinant forms of myc-tagged viral Pellino and Pellino3S (1 μg) were incubated with ubiquitin (1 μg), in the presence and absence of E1 (50 ng) and heterodimeric E2 UbcH13/Uev1a (400 ng) for 2 h at 37°C. Reactions were terminated by addition of SDS-PAGE sample buffer. Samples were subjected to PAGE and subsequently to Western immunoblotting using anti-ubiquitin and anti-myc antibodies. The arrow indicates myc-tagged viral Pellino.

Pellino family were initially characterised as scaffold proteins that regulate TLR-mediated activation of NF-κB and MAPKs [10, 11]. More recently, Pellinos have been shown to function as E3 ubiquitin ligases, catalysing K63-linked polyubiquitination of IRAK-1 [14–16]. Indeed there exists a bidirectional communication in the IRAK–Pellino associations, in that IRAK-1 and IRAK-4

can phosphorylate Pellino proteins on various serine and threonine residues, thus enhancing the E3 ubiquitin ligase activity of the Pellinos. The latter can then catalyse polyubiquitination of IRAK-1 [16, 17]. The C-terminal regions of the Pellino proteins contain a conserved RING-like domain that confers E3 ubiquitin ligase activity. Furthermore, the recent resolution of the x-ray structure of a N-terminal fragment (amino acids 15–275) of Pellino2 that lacks the RING-like domain, revealed a cryptic forkhead-associated (FHA) domain that was not apparent from the primary structure [18]. The FHA domain is a phospho-threonine-binding module and underlies the ability of Pellino proteins to interact with phosphorylated IRAK-1. The FHA domain in the Pellino family differs from the classical FHA domain present in other proteins by containing an additional appendage or "wing" that is formed by two inserts in the FHA region [18]. Although the importance of this appendage region for IRAK binding remains to be experimentally addressed, it is worth noting that multiple IRAK phosphorylation sites reside in the "wing" region [17].

Intriguingly, a viral form of Pellino has been previously identified as an open reading frame (ORF) from the genome of *Melanoplus sanguinipes* entomopoxvirus (MsEPV) [19, 20]. The genomic location of this ORF near the right-hand side inverted terminal repeat indicates that viral Pellino could possess an immunomodulatory function [19]. The conceptual translation of the viral Pellino ORF has been shown to display sequence similarity to human, insect and nematode Pellino proteins [19, 20], suggesting that viral Pellino is a homolog of genes encoding receptor proximal intracellular signalling proteins in the Toll and TLR pathways. This prompted us to perform a functional characterisation of the regulatory effects of viral Pellino in these pathways. We demonstrate that viral Pellino can down-regulate Toll-mediated activation of the *Drosophila* antimicrobial response and inhibit human TLR signalling to NF-κB, underscoring the importance of Pellinos within this signalling axis in the innate immune system.

Results

Homology modelling of viral Pellino

The amino acid sequence and the two available structures of Pellino2 (PDB: 3EGA at 1.8 Å and 3EGB at 3.3 Å) [18] were used as templates for comparative modelling of viral Pellino. An initial alignment between the full amino acid sequence of Pellino2 and the viral Pellino resulted in a poor overall sequence identity of 15.6% (http://www.ebi.ac.uk/). This sequence identity rises to 16.5% (26.4% similarity) if the two insert regions (residues 51–98 and 159–184) that form the non-canonical wing decoration of the FHA domain in Pellino2 are excluded from the alignment. Indeed, when just considering an alignment of the FHA domain region of the Pellino2 crystal structures, a sequence identity of 27.6% to the 3EGA crystal structure sequence and 25.5% to the 3EGB crystal structure sequence was observed

(Fig. 1A). Modeller 9v5 [21] was used to generate multiple models from both available templates of Pellino2 to examine the structure and stability of viral Pellino modeled as an FHA domain. The best model was selected using a combination of the Modeller objective function score and a stereochemical analysis using ProCheck [22, 23] with only one outlier being identified. Subsequently, the model was minimised using MOE 2008 (http://www.chemcomp.com) in a 5 Å water sphere using the Amber99 force field to further examine its stability. Following this process, a stable 11-stranded β-sandwich remained for viral Pellino (Fig. 1B). A topology-based comparison with Pellino2 demonstrates that the β-sandwich has the same strand orientation as that observed for the core FHA domain of Pellino2. To further assess the stability of our developed model, it was subjected to a 5 ns molecular dynamics simulation with a maximum root mean square deviation (RMSD) of 3.5 Å being experienced. An average structure was taken over the last 2 ns of simulation and upon examination of the secondary structure elements the 11-stranded β-sandwich had remained intact. This comparative model of viral Pellino superimposes well on the crystal structure of the Pellino2 FHA core region (Fig. 1C).

This suggests that viral Pellino has the potential to form a core FHA domain without the wing appendage that is present in Pellino2. The lack of a wing appendage means that viral Pellino lacks the multiple IRAK phosphorylation sites present in Pellino2. However, viral Pellino contains most of the highly conserved signature amino acid residues that are found in canonical FHA domains and that are required for binding to phosphorylated peptides and proteins. These five crucial residues in Pellino2 are R106, S137, R138, T187 and N188 [18] and correspond to R33, S47, N48, Q85 and N86 in viral Pellino. Thus, viral Pellino contains four of the five highly conserved residues in classical FHA domains that are required for binding to phosphorylated protein-binding partners. This, in conjunction with the homology modeling described above, provides strong predictive indication that viral Pellino contains a core FHA domain.

The ability of mammalian Pellinos to function as E3 ubiquitin ligases is bestowed by the presence of a C-terminal RING domain, where the eight cysteine and histidine residues are arranged in the atypical CHC2CHC2 formation. This RING domain is conserved between mammalian, nematode and *Drosophila* Pellinos. However, alignment of the C-terminal regions of these Pellino sequences with that of poxviral Pellino shows that the viral protein possesses a partial RING domain containing only the second CGH triplet and CPXC motif (Fig. 1D). This partial RING domain is insufficient to confer E3 ubiquitin ligase activity on viral Pellino since a recombinant form of the latter failed to catalyse the in vitro generation of polyubiquitin chains in the presence of E1 and E2 enzymes, whereas the mammalian member Pellino3S shows strong catalytic activity (Fig. 1E). Western immunoblotting using an anti-myc antibody shows that the lack of activity of viral Pellino relative to Pellino3 cannot be attributed to differences in protein quantity since both proteins show comparable levels of immunoreactivity. Interestingly, viral

Pellino has a mobility corresponding to its predicted size of 25.4 kDa but it also shows a fainter immunoreactive band of slower electrophoretic mobility. The identity of this protein is unknown but its lack of reactivity with the anti-ubiquitin antibody excludes the possibility of the protein being modified by ubiquitination. The above analysis suggests that viral Pellino resembles its mammalian counterparts in containing a core FHA domain but differs in lacking both a wing appendage to the FHA domain and a functional RING-like motif.

Viral Pellino inhibits Toll- and TLR-triggered signalling responses

The emerging roles of Pellino proteins in TLR signalling coupled to the discovery of a viral homolog prompted studies on the ability of viral Pellino to regulate TLR signal transduction. Viral Pellino is encoded by the genome of MsEPV and given that the natural host of MsEPV is insect cells, the highly AT-rich sequence of the viral Pellino gene reflects an adaptation to this environment. In order to ensure expression of viral Pellino in both insect and human cells, a form of the gene was chemically synthesised with codon sequences optimised for recognition by human translation machinery. This involved replacing As or Ts in the third position of each codon with a G or C, without altering the amino acid sequence of the translated protein. Such an approach was previously shown to enhance expression of poxviral genes in human cells [24].

We initially assessed the effects of viral Pellino on Toll signalling in macrophage-like *Drosophila* S2 cells. A myc-tagged version of the viral protein showed uniform cytoplasmic distribution after transfection in these cells (Fig. 2A). The effects of increasing levels of viral Pellino expression on signalling by the Toll ligand C-106 was then assessed (Fig. 2B). C-106 is the active C-terminal fragment of the Spätzle protein and induced activation of a firefly luciferase reporter under the control of the *drosomycin* promoter. Toll signalling can induce expression of this antimicrobial peptide through the Rel family transactivators Dorsal and Dif. Thus, the activation of the *drosomycin* promoter was an especially relevant readout for Toll signalling in the present studies in light of the demonstration that *Drosophila* Pellino plays a key role in driving expression of drosomycin [13]. Expression of increasing levels of viral Pellino caused a dose-dependent inhibition of C-106-induced activation of the *drosomycin* promoter. This inhibitory effect was confirmed in S2 cells stably expressing viral Pellino following lentiviral transduction. Viral Pellino also displayed cytoplasmic localisation upon stable expression (Fig. 2C) and inhibited C106-induced activation of the *drosomycin* promoter (Fig. 2D). This confirms that the entomopoxviral protein can obstruct a key insect immune–response pathway.

The high degree of sequence and mechanistic conservation between insect Toll and mammalian TLR signalling pathways led us to further explore the potential immunomodulatory capabilities of viral Pellino in human cells. Expression of

increasing amounts of viral Pellino in HEK293-TLR4 cells (Fig. 3A) showed dose-dependent inhibition of LPS-induction of an NF-κB-responsive promoter–reporter construct (Fig. 3B). We next confirmed that viral Pellino could block the endogenous NF-κB pathway in a cell that was naturally responsive to LPS by demonstrating that lentivirally delivered viral Pellino blocked the LPS-induced phosphorylation of the NF-κB subunit p65 upon stable expression in U373 cells (Fig. 3C). The regulatory effects of viral Pellino on the NF-κB pathway have functional consequences for pro-inflammatory gene expression since the transduction of THP-1 monocytic cells with varying titres of lentivirus, conferring stable viral Pellino expression, caused an inhibition of LPS induced expression of the NF-κB-responsive gene IL-8 (Fig. 3D). The highest titre also inhibited LPS induction of TNF in THP-1 cells (Fig. 3E). These studies confirm the regulatory effects of viral Pellino on TLR4 signalling in a number of cell types.

Viral Pellino interacts with IRAK-1 in a kinase-independent but FHA-dependent manner

We next investigated the mechanistic basis to the regulatory effects of viral Pellino on TLR signalling. IRAK-1 was an obvious target for viral Pellino, given that the mammalian Pellinos have been shown to associate with IRAK-1 [10, 25], probably via their FHA domain, and that the homology modelling studies detailed above suggest the presence of a core FHA domain in viral Pellino. Co-immunprecipitation studies demonstrated that vPellino and IRAK-1 associated upon co-expression. This was observed upon immunoprecipitation of viral Pellino and immunoblotting for IRAK-1 (Fig. 4A). Furthermore, viral Pellino was found to interact with endogenous IRAK-1 upon immunoprecipitation of the latter (Fig. 4B). The IRAK-1-viral Pellino interaction is also apparent under conditions where viral Pellino is expressed at more physiologically relevant levels as facilitated by lentiviral-mediated delivery of viral Pellino into U373 cells (Fig. 4C). Further evidence in support of the IRAK-1-Pellino interaction is provided by co-localisation of IRAK-RFP and viral Pellino-GFP in HEK293 cells (Fig. 4D).

Conflicting reports exist on the importance of IRAK-1 kinase activity in the interaction between mammalian Pellinos and IRAK-1 [14, 15]. Kinase activity does not appear to be required for interaction with viral Pellino, as a kinase-dead form of IRAK-1 (IRAK-1-KD, K239A) also co-immunoprecipitated with myc-tagged viral Pellino (Fig. 4E, upper panel). Kinase-active members of the IRAK family, IRAK-1 and IRAK-4, have been shown to induce the degradation of mammalian Pellinos in a kinase-dependent fashion [15]. This type of regulation is retained in the interaction between IRAK-1 and viral Pellino, as reduced levels of the latter are apparent when co-expressed with IRAK-1, but not IRAK-1-KD (Fig 4A, B versus E).

The ability of viral Pellino to interact with IRAK-1 supports our homology modelling studies that predicted viral Pellino capable of forming a FHA domain. In order to directly address the potential
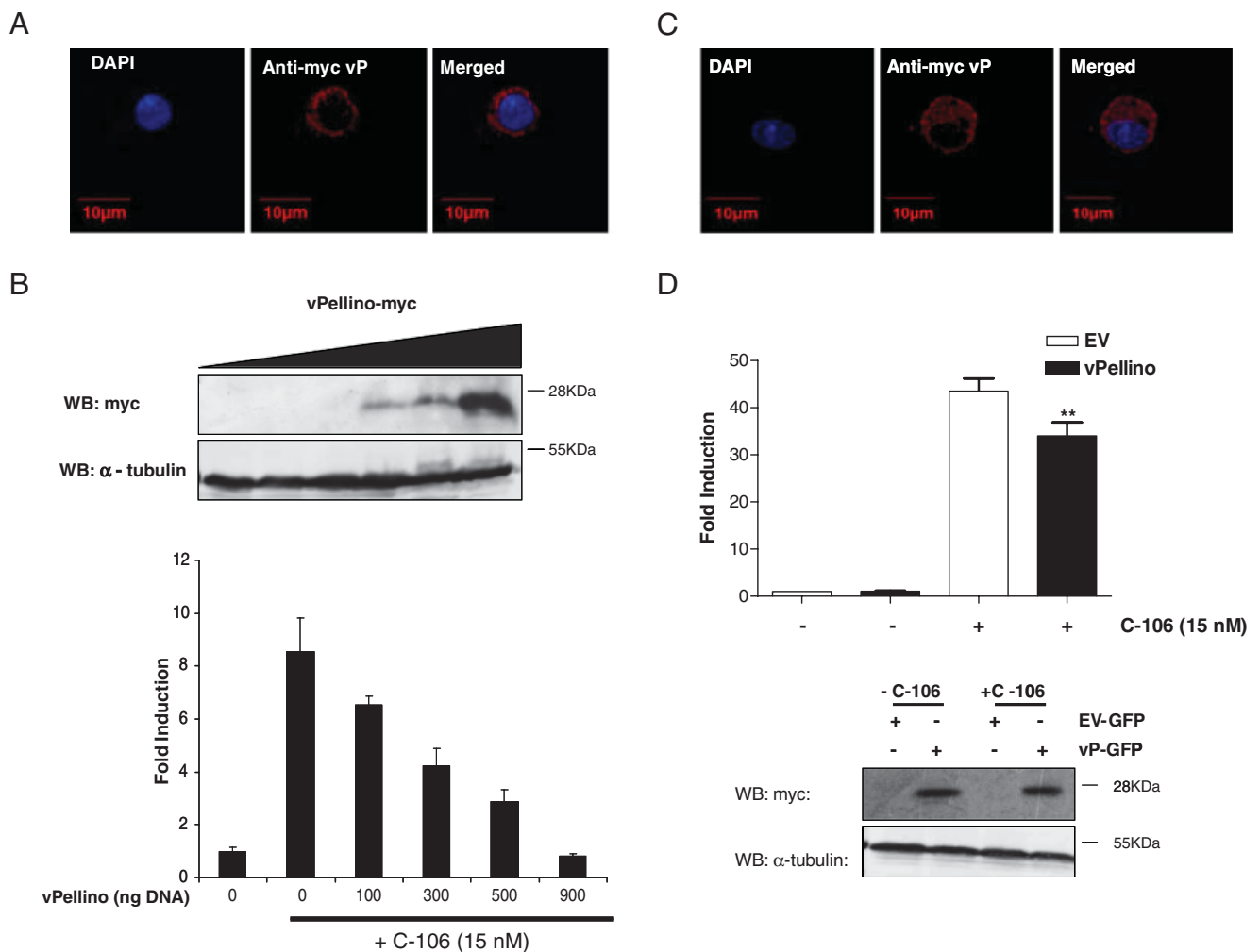
A

| DAPI | Anti-myc vP | Merged |

B

vPellino-myc

WB: myc — 28KDa

WB: α - tubulin — 55KDa

C

| DAPI | Anti-myc vP | Merged |

D

- C-106   +C -106

| + | - | + | - | EV-GFP |
| - | + | - | + | vP-GFP |

WB: myc: — 28KDa

WB: α-tubulin: — 55KDa

Figure 2. Viral Pellino inhibits *drosomycin* promoter activation by C-106. (A, B) *Drosophila* S2 cells were co-transfected with *drosomycin* promoter-luciferase (20 ng), Ach110-β-galactosidase (80 ng) and with/without varying amounts of myc-tagged viral Pellino. (C, D) *Drosophila* S2 cells were stably transduced with control or myc-tagged viral Pellino lentivirus. 72 h later cells were co-transfected with *drosomycin* promoter-luciferase (20 ng) and Ach110-β-galactosidase (80 ng). (A, C) Sub-cellular localisation of viral Pellino was visualised by immunohistochemical analysis using a combination of anti-myc antibody and an Alexa fluor 594 anti-mouse secondary antibody (Invitrogen). DAPI was used to stain nuclei. Images are representative of two independent experiments. (B, D) After transfection, cells were stimulated overnight in the presence/absence of C-106 (15 nM). (B, D) Lysates were subjected to anti-myc and anti-α-tubulin immunoblotting. (B, D) Lysates were assayed for firefly luciferase and β-galactosidase activity. Data are presented as fold induction of normalised luciferase activity relative to unstimulated cells. (B) Representative of three independent experiments performed in triplicate. (D) Data were subjected to one-way ANOVA statistical analysis. **$p<0.01$; C106-treated cells transduced with control lentivirus versus C106-treated cells transduced with equivalent titre of vPellino. Results represent mean+S.E.M. of three independent experiments, each performed in triplicate.

importance of the putative FHA domain of viral Pellino in facilitating its interaction with IRAK-1, truncation mutants of viral Pellino were generated that lack the first 90 (ΔF1-myc) or 50 (ΔF2-myc) amino acid residues. These mutants were designed based on the former lacking all five of the conserved residues that signature a classical FHA domain and the latter lacking the first three of these conserved residues. Unlike full-length viral Pellino, the truncation mutants, lacking the first 50 or 90 residues, failed to interact with IRAK-1 (Fig. 5A, upper panel). These studies are again consistent with viral Pellino containing a FHA domain that makes a critical contribution to enabling viral Pellino to interact with IRAK-1. The interaction of IRAK-1 with the shorter spliced form of human Pellino 3 (P3S) served as a positive control for this analysis.

The above truncation mutants were also exploited to evaluate the importance of IRAK-1 binding for manifesting the inhibitory effects of viral Pellino on TLR signalling. As described above, full-length viral Pellino was again shown to cause a dose-dependent inhibition of LPS-induced activation of NF-κB (Fig. 5B). The removal of the first 50 or 90 residues from viral Pellino failed to fully abolish its ability to inhibit LPS signalling. As the removal of the first 50 residues from viral Pellino abolished its ability to bind IRAK-1 but had no effect on its negative regulatory potential, a more refined approach was performed to further define the functional importance of the putative FHA domain of viral Pellino. Interestingly, the truncation of the first 50 amino acids includes removal of the highly conserved FHA-signature residues R33 and
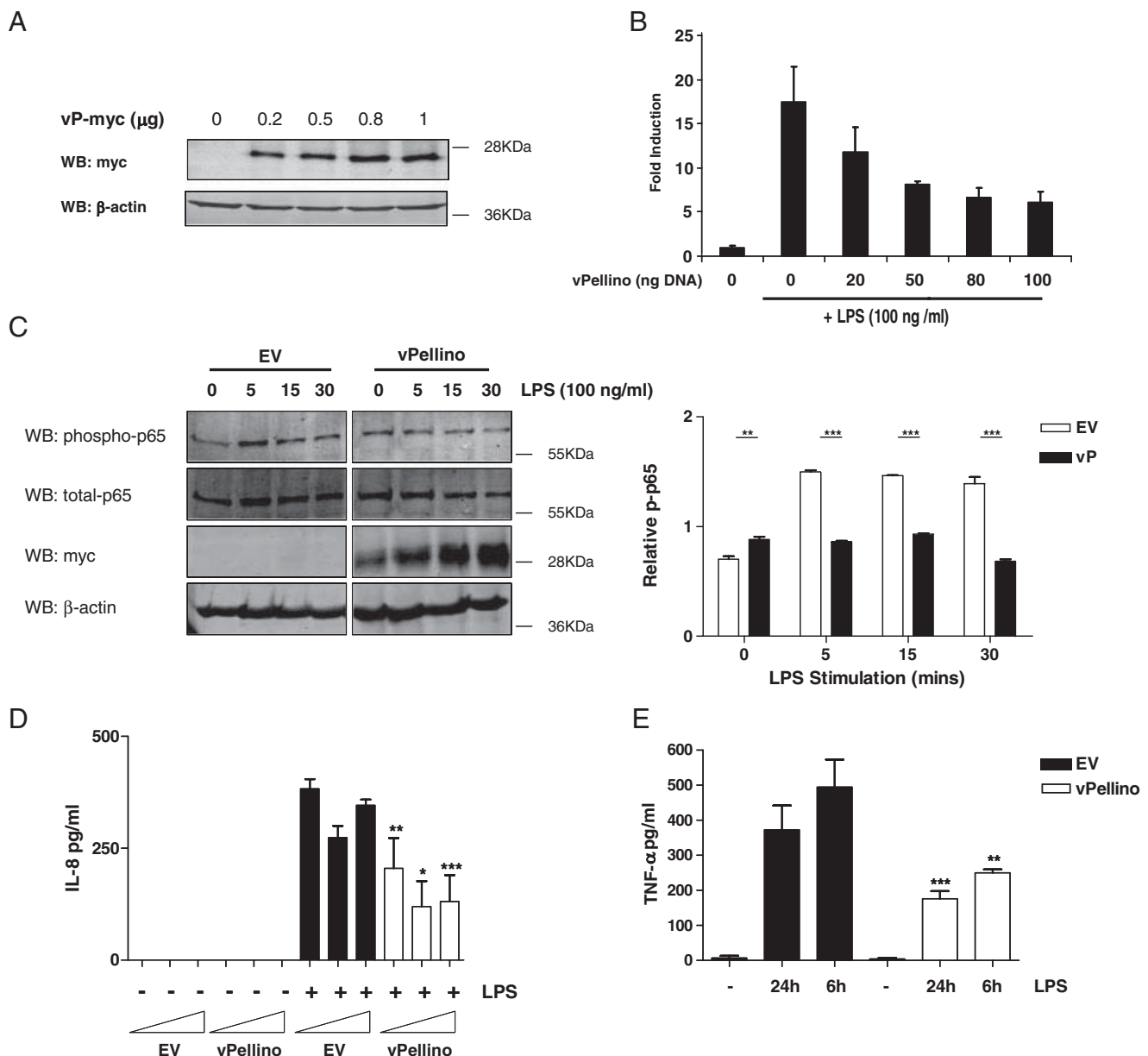
Figure 3. Viral Pellino inhibits TLR signal transduction. HEK293-TLR4 cells were co-transfected with NF-κB-luciferase (80 ng) and pGL3-*Renilla* luciferase (20 ng) and with/without (A) 0–1 μg or (B) 0–100 ng myc-tagged viral Pellino. (A) Lysates were subjected to PAGE and anti-myc and anti β-actin immunoblotting. (B) Cells were stimulated with/without LPS (100 ng/mL) 8 h before harvesting. Lysates were assayed for firefly and pGL3-*Renilla* luciferase activity. Data are representative of three independent experiments and are presented relative to cells transfected with empty vector alone. (C) U373 cells stably transduced with control or viral Pellino lentivirus were treated with LPS (100 ng/mL) for indicated timepoints. Lysates were subjected to immunoblotting using anti-phospho-p65, anti-total-p65, anti-myc and anti-β-actin antibodies. Resulting images of phospho-p65, from three independent experiments, were subjected to densitometric analysis (normalised to total p65) and subject to Student's *t*-test. ***$p < 0.001$, **$p < 0.01$. (D) THP-1 cells were transduced with 1×10^5, 2×10^5 and 3×10^5 or (E) 3×10^5 transducing units (TU) of control or viral Pellino lentivirus. After 72 h, cells were treated with LPS (100 ng/mL) for 24 h. Conditioned media were harvested and assayed for levels of (D) IL-8 and (E) TNF by ELISA. Data were subjected to one-way ANOVA statistical analysis. ***$p < 0.001$, **$p < 0.01$, *$p < 0.05$; LPS-treated cells transduced with EV versus LPS-treated cells transduced with equivalent titre of viral Pellino lentivirus. Results represent mean+S.E.M. of three independent experiments, each performed in triplicate.

S47. Each of these two residues was independently mutated to alanine and the functional properties of the resulting point mutants examined. The substitution of either residue by alanine removed the ability of viral Pellino to interact with IRAK-1 (Fig. 5C), but yet did not eliminate its ability to inhibit LPS-induced activation of NF-κB (Fig. 5D). These findings suggest that the putative FHA domain of viral Pellino is important for IRAK-1 binding but is dispensable for manifesting the inhibitory effects on LPS signalling. This suggests that viral Pellino may target signalling molecules other than IRAK-1 in its regulation of TLR signalling.
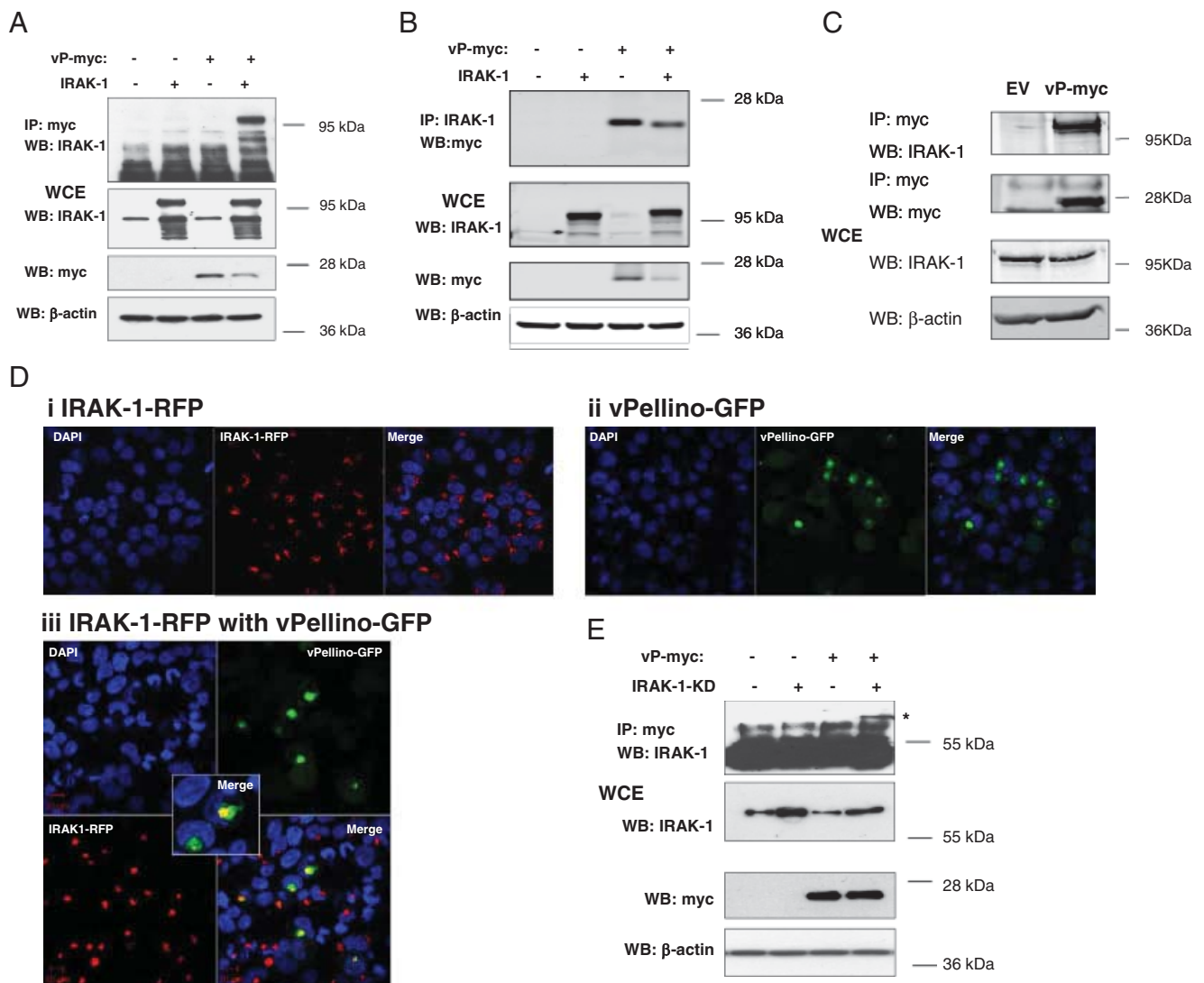
Figure 4. Viral Pellino interacts with IRAK-1 in a kinase-independent manner. (A, B, E) HEK293 cells were co-transfected with expression constructs encoding myc-tagged viral Pellino or pcDNA empty vector (3 μg) and an (A) IRAK-1 or (E) IRAK-1-KD expression construct (1 μg). Lysates were generated after 24 h, immunoprecipitated with an (A, E) anti-myc antibody or (B) an anti-IRAK antibody, and subsequently immunoblotted using designated antibodies. Lysates were analysed by immunoblotting using anti-IRAK-1, anti-myc and anti-β-actin antibodies. (E) An asterisk (*) indicates the position of the co-immunoprecipitated IRAK-1-KD band and the data are representative of two independent experiments. (C) U373 cells were transduced with control or viral Pellino lentivirus. Lysates were generated after 24 h, immunoprecipitated with an anti-myc antibody and subsequently immunoblotted using anti-IRAK and -myc antibodies. Lysates were also immunoblotted for IRAK and β-actin. (D) HEK293T cells were co-transfected with expression constructs encoding (i) IRAK-RFP, (ii) viral Pellino-GFP or (iii) IRAK-RFP and viral Pellino-GFP fusion proteins. Confocal images were captured using the ×63 objective (oil immersion) on the UV Zeiss 510 Meta System laser-scanning microscope equipped with the appropriate filter sets and analyzed using the LSM 5 browser imaging software. All data are representative of three independent experiments, unless otherwise stated.

Pellino3S is functionally antagonised by viral Pellino

The co-immunoprecipitation of viral Pellino with IRAK-1 raised the possibility that the viral protein could compete with signalling intermediates for association with IRAK-1. Given the homologous nature of viral Pellino to the mammalian Pellino family, coupled to the IRAK-binding capacity of members of the latter, it was intriguing to explore the impact of viral Pellino expression on the interaction between mammalian Pellino proteins and IRAK-1. Pellino3S was used as a representative of the mammalian Pellino family. Co-immunoprecipitation analysis confirmed a strong association between Pellino3S and IRAK-1, but this interaction was eliminated upon co-expression of viral Pellino (Fig. 6A, upper panel). In addition, the interaction of Pellino3 with kinase-dead IRAK-1 was also reduced in the presence of viral Pellino (Fig. 6B, upper panel). Furthermore, immunoblotting whole-cell lysates for IRAK-1 demonstrated that the post-translational modification of IRAK-1 seen in response to Pellino3S expression was partially reduced with addition of viral Pellino (Fig. 6A, second panel, compare lanes 7 and 8). This disruption of
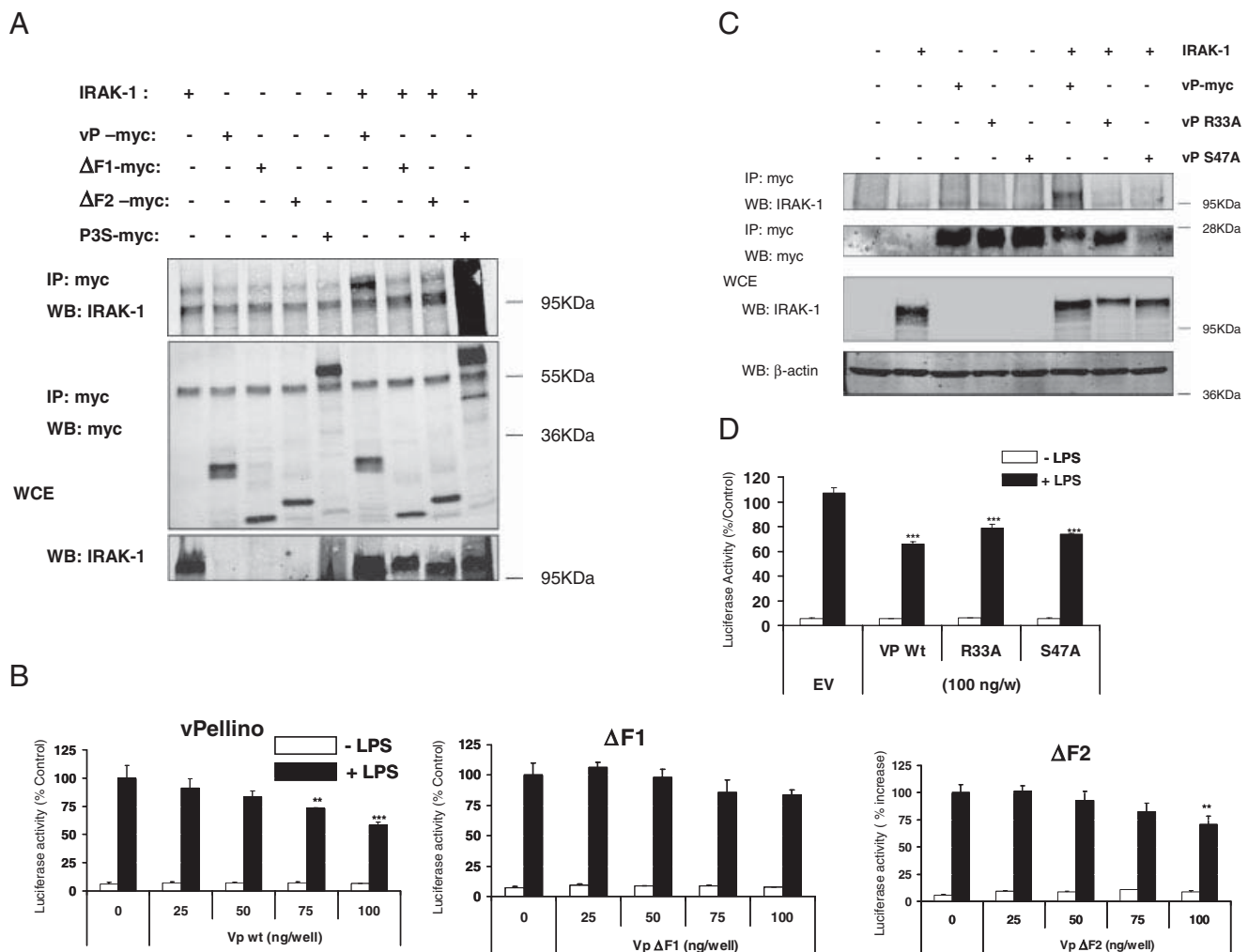
Figure 5. Functional characterisation of putative FHA domain of viral Pellino. (A, C) HEK293 cells were co-transfected with expression constructs encoding myc-tagged full-length viral Pellino (vP), residues 90–203 of viral Pellino (ΔF1), residues 50–203 of viral Pellino (ΔF2), viral Pellino with point mutations of residue 33 from R to A (R33A) or residue 47 from S to A (S47A), human Pellino3S (P3S) construct or pcDNA empty vector (3 μg) and with/without an IRAK-1 expression construct (1 μg). Lysates were generated after 24 h, immunoprecipitated with an anti-myc antibody and subsequently immunoblotted using anti-IRAK antibodies. Lysates were analysed by immunoblotting using anti-IRAK-1, anti-myc and anti-β-actin antibodies. Data are representative of three independent experiments. (B, D) HEK293-TLR4 cells were co-transfected with NF-κB–luciferase (80 ng) and pGL3-*Renilla* luciferase (20 ng) and with or without indicated amounts of vP, ΔF1, ΔF2, R33A or S47A. Cells were stimulated with or without LPS (100 ng/mL) 8 h before harvesting. Lysates were assayed for firefly and pGL3-*Renilla* luciferase activity. Data are presented relative to stimulated cells transfected with empty vector alone. (B) Data were subjected to one-way ANOVA statistical analysis, **$p<0.01$, ***$p<0.001$ comparing the level of LPS-induced reporter gene activity observed in the presence of viral Pellino WT and mutant proteins to that observed with LPS in control cells. Results represent mean±S.E.M. of three independent experiments. (D) Data were subjected to a two-tailed paired *t*-test. Results represent mean±S.E.M. of three independent experiments.

Pellino3S-IRAK-1 complexes and inhibition of Pellino3S-mediated IRAK-1 modification was likely due to the enhancement of Pellino3S degradation apparent with viral Pellino co-expression (Fig. 6A, third panel). This accelerated degradation of Pellino3S was dependent on IRAK-1 kinase activity, as it was not observed upon substitution of IRAK-1-KD for WT IRAK-1 (Fig. 6B). The depletion of Pellino3S in the presence of viral Pellino displays some degree of specificity since the latter fails to deplete the expression of control GFP protein (data not shown).

An ability to promote degradation of Pellino3S would imply that viral Pellino can functionally inhibit the mammalian protein. Pelli-no3S is known to regulate activation of MAPKs [26]. We therefore monitored the effect of the viral protein on Pellino3S-mediated activation of p38 MAPK. HEK293 cells were co-transfected with or without viral Pellino and Pellino3S and with components of the PathDetect™ CHOP *trans*-Reporting System that measures activation of p38 MAPK. Reporter activity was induced upon expression of Pellino3S (Fig. 7A). However, co-expressing viral Pellino inhibited Pellino3S-mediated up-regulation of CHOP transactivation, an index of p38 MAPK activity. To further validate these findings, another assay of p38 MAPK kinase activity was employed. The latter is known to phosphorylate the downstream kinase MAPKAP kinase 2
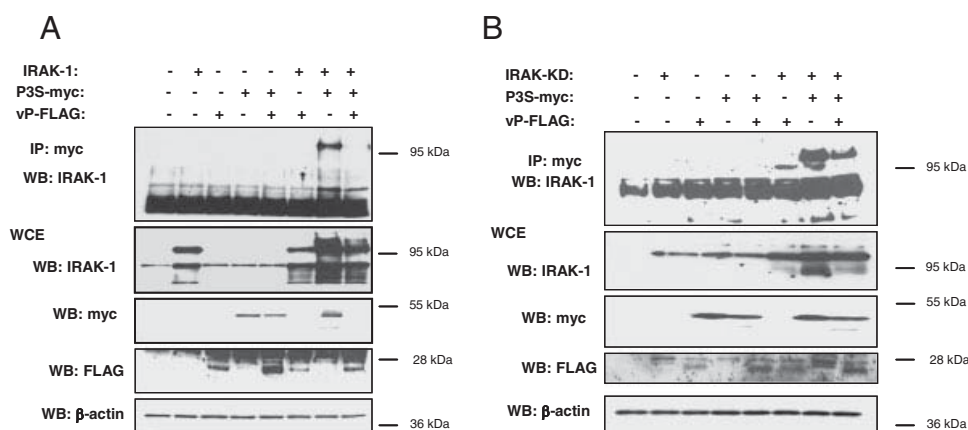
Figure 6. Viral Pellino targets a mammalian counterpart. HEK293 cells were co-transfected with or without Pellino3S-myc, viral Pellino-FLAG and either (A) IRAK-1 or (B) IRAK-1-KD. Lysates were immunoprecipitated with an anti-myc antibody. Immunoprecipitates were subjected to PAGE and anti-IRAK-1 immunoblotting. Lysates were analysed by immunoblotting using anti-IRAK-1, anti-myc, anti-FLAG and β-actin antibodies. Data are representative of (A) three and (B) two independent experiments.
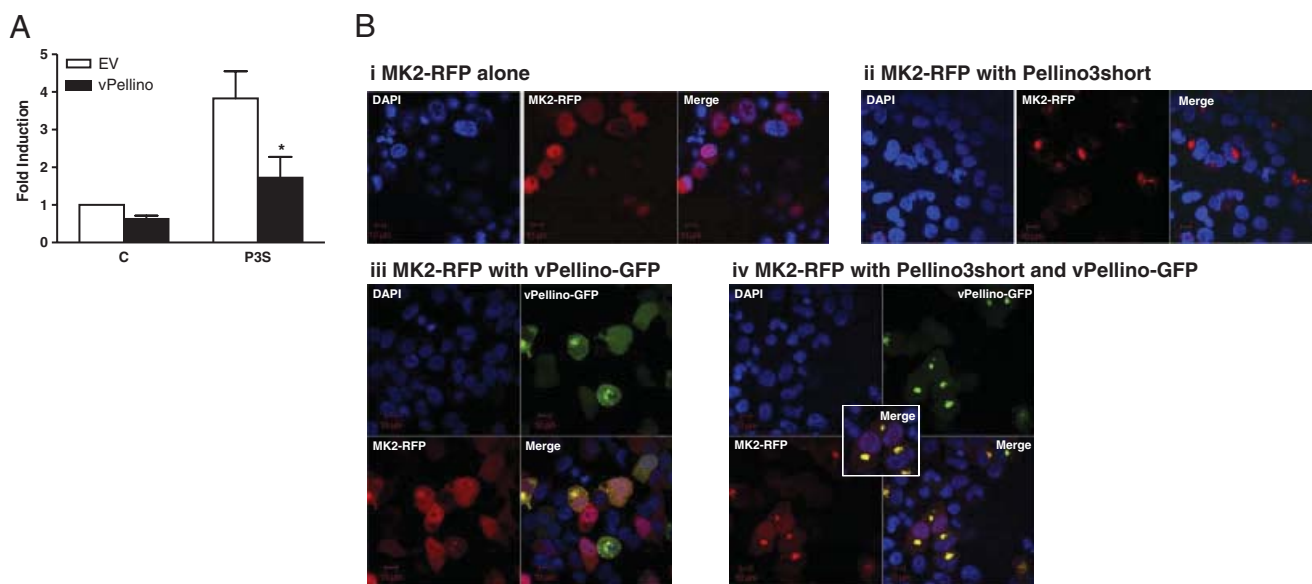

Figure 7. Viral Pellino inhibits Pellino3-mediated activation of the p38 MAPK pathway. (A) HEK293 cells were co-transfected with pFA-CHOP, pFR-luciferase, pGL3-*Renilla* luciferase and with or without plasmids encoding Pellino3S and viral Pellino. Lysates were assayed for firefly and *Renilla* luciferase activity. Data are presented relative to cells transfected with empty vector alone and were subjected to a paired *t*-test. The asterisk (*) indicates that viral Pellino reduces Pellino3S-induced up-regulation of CHOP transactivation with $p < 0.05$. Results represent mean + S.E.M. of three independent experiments, each performed in triplicate. (B) HEK293 cells were co-transfected with MAPKAP kinase 2-Ds Red and (i) pcDNA3.1 empty vector (ii) Pellino3S (iii) viral Pellino-GFP or (iv) Pellino3S and viral Pellino-GFP. Confocal images were captured using the ×63 objective (oil immersion) on the UV Zeiss 510 Meta System laser-scanning microscope equipped with the appropriate filter sets and analysed using the LSM 5 browser imaging software. (iii) and (iv) The upper left panels indicate DAPI staining of the nuclei. The upper right panels represent images of isolated viral Pellino-GFP fluorescence. The lower left panels indicate images of isolated MAPKAP kinase 2-Ds Red fluorescence. The lower right panels are montages of the three other images. Captured images are representative of three independent experiments.

and promote its re-distribution from the nucleus to the cytoplasm. Pellino3S was shown to affect nuclear-cytoplasmic shuttling of a RFP tagged form of MAPKAP kinase 2 with all of the latter exiting the nucleus in the presence of Pellino3S (Fig. 7B). However, the co-expression of a GFP tagged form of viral Pellino inhibited Pellino3S-mediated cytoplasmic shuttling of MAPKAP kinase 2 resulting in considerable residual levels of the latter remaining in the nucleus. These findings demonstrate that the poxviral protein can negatively affect signalling from a mammalian counterpart.

Association of viral Pellino with TIR-containing adaptor proteins

Given that viral Pellino can functionally antagonise its mammalian counterparts and the latter has been demonstrated to participate in multiprotein signalling complexes [14, 27], we next examined the functional regulation of other TLR signalling molecules by viral Pellino. Components of the TLR/NF-κB pathway were expressed at levels sufficient to induce NF-κB

activation. Co-expression of viral Pellino led to a substantial inhibition of reporter gene activity mediated by the TIR-containing adaptor proteins MyD88 and Mal (Fig. 8A), whereas TRIF- and TRAM-mediated activation of NF-κB was less sensitive to viral Pellino (data not shown). The poxviral protein also displayed inhibitory activity towards NF-κB activation by downstream TLR signalling pathway components IRAK-1, TRAF6 and IKKβ but not p65 (Fig. 8A). The lack of effect of viral Pellino on p65 suggests specificity of action for viral Pellino, albeit with multiple targets. The regulation of a number of these signalling molecules by viral Pellino is consistent with its functional antagonism of mammalian Pellinos. Since Pellinos interact with IRAK-1 and TRAF-6 and promote polyubiquitination of IRAK-1 that subsequently recruits IKK-containing complexes, it is not surprising that viral Pellino-induced degradation of mammalian Pellinos negatively regulates IRAK-1, TRAF6 and IKKβ. However, viral Pellino also showed inhibitory potential upstream of IRAK-1 in functional assays, suggesting that viral Pellino targets signalling molecules beyond IRAK-1. Indeed, this is further corroborated by our earlier findings demonstrating that truncation mutants of viral Pellino, lacking a FHA domain, fail to interact with IRAK-1 and yet partially retain

inhibitory effects on TLR signalling. We thus next investigated other potential targets for viral Pellino and more specifically probed whether it could also interact with the TIR adaptor proteins, MyD88 and Mal, given their sensitivity to viral Pellino. Co-immunoprecipitation studies demonstrated that viral Pellino can associate with MyD88 (Fig. 8B, upper panel) and Mal (Fig. 8C, upper panel). Interestingly, in the case of both adaptors, interaction with viral Pellino led to reduced levels of adaptor protein (Fig. 8B and C, second panels). Such effects on the expression levels of the adaptor proteins were observed reproducibly and appear to represent some degree of specificity, given that viral Pellino fails to affect the expression levels of co-expressed IRAK-1 (Fig. 4A and B). The lack of an intact RING domain eliminates the possibility that viral Pellino itself can directly induce polyubiquitination and subsequent degradation of TLR signalling components, suggesting that it may recruit an intermediary protein capable of such regulation. Indeed, the C-terminal region containing the partially conserved RING domain is not required for the inhibitory function of viral Pellino since a deletion mutant lacking the C-terminal CHC2 and CGH residues retained a comparable ability to the WT protein towards
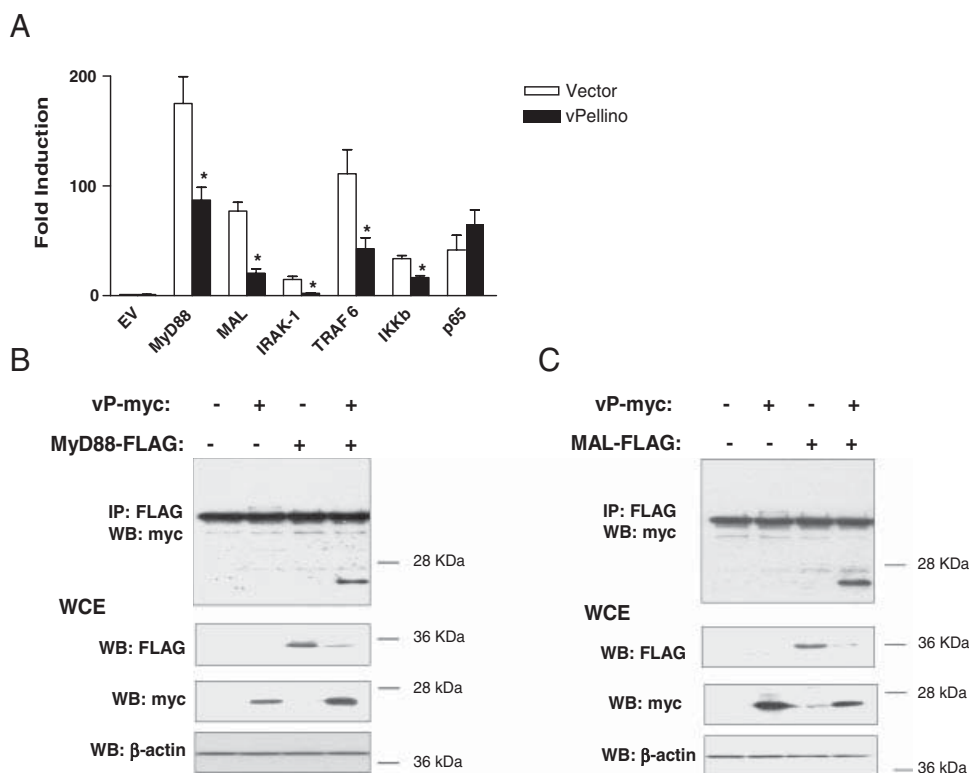

Figure 8. Viral Pellino immunoprecipitates with TIR adaptor proteins. (A) HEK293-TLR4 cells were co-transfected with empty expression vector (EV) or constructs encoding MyD88, Mal, IRAK-1, TRAF6, IKKβ or p65 and NF-κB-luciferase (80 ng) and pGL3-*Renilla* luciferase (20 ng) and with or without viral Pellino (80 ng). In total, 24 h post-transfection, lysates were assayed for firefly and pGL3-*Renilla* luciferase activity. Data are presented relative to cells transfected with empty vector alone and were subjected to a paired *t*-test. The asterisk (*) indicates that viral Pellino reduces the corresponding TLR-signalling component-induced NF-κB activation with $p < 0.05$. Results represent mean + S.E.M. of three independent experiments, each performed in triplicate. (B, C) HEK293 cells were co-transfected with/without plasmids encoding myc-tagged viral Pellino and (B) FLAG-tagged MyD88 or (C) Mal. Lysates were generated after 24 h and immunoprecipitated with an anti-FLAG antibody. Immunoprecipitates were subjected to anti-myc immunoblotting. A heavy-chain-specific anti-mouse secondary antibody was used as myc-tagged viral Pellino electrophoretically co-migrates with antibody light chains. Cell lysates were analysed by immunoblotting using anti-FLAG, anti-myc and anti-β-actin antibodies. Data are representative of two independent experiments.

reducing levels of Mal protein and towards inhibition of Mal-mediated activation of NF-κB (data not shown). Irrespective of the exact mechanism, the targeting of TIR adaptor proteins may represent a further mechanism underlying the inhibitory effects of viral Pellino on TLR signalling.

Discussion

Viruses have evolved a wide range of immunoevasive strategies, including the targeting of key innate immune signalling pathways. Vaccinia virus A52R has been shown to inhibit TLR-mediated activation of NF-κB by disrupting signalling complexes containing TRAF6 and IRAK2 [28]. Furthermore, in a manner similar to the actions of viral Pellino on IRAK-1, MCMV M45 was found to bind RIP1, blocking its ubiquitination and thereby activation of NF-κB by TNF-α and TLR3 signalling [29]. Here, we reveal the immunoevasive properties of a poxviral Pellino homolog. This identifies the ability of an entomopoxvirus protein to combat insect immunity. The ability of viral Pellino to also interfere with TLR signalling highlights the amazing conservation across the evolutionary divide of Toll and TLR signalling. An increased understanding of the mechanistic basis to the regulatory effects of viral Pellino may also provide a greater appreciation of the precise role of mammalian Pellinos in IL-1/TLR signalling.

Viral Pellino was initially discovered based on the sequence identity with members of the mammalian Pellino family. However, the sequence identity was quite low and given that the X-ray structure of part of the Pellino2 protein had been recently resolved, we employed homology modelling to evaluate if the limited sequence identity has the potential to translate into shared structural properties. An intriguing picture emerges in which viral Pellino shares some of the structural characteristics of mammalian proteins but differs in other respects. Like some of its mammalian counterparts, it has a cytoplasmic localisation. This is hardly surprising since bioinformatic analysis failed to predict any transmembrane domain or nuclear localisation sequences. Mammalian Pellinos possess two distinct domains; a N-terminal FHA domain that facilitates binding to phosphorylated IRAK-1 [18] and a C-terminal RING-like domain that catalyses poly-ubiquitination of IRAK-1. Viral Pellino lacks the latter but appears to have the potential to form a FHA domain based on two sets of findings. First, homology modelling in conjunction with molecular dynamics indicates the potential for viral Pellino to form a stable 11-stranded β-sandwich that is characteristic of a canonical FHA domain. Second, viral Pellino shows conservation of the four signature amino acid residues in FHA domain-containing proteins that mediate direct binding to phosphorylated threonine residues on partner proteins. Interestingly, the putative FHA domain in viral Pellino appears to be a core FHA domain that lacks the two insert regions in mammalian Pellinos that decorate their FHA domains with a wing appendage. Thus, viral Pellino is a valuable experimental tool that enables one to evaluate the importance of the wing region in the Pellino FHA domain for IRAK binding. Since viral Pellino retains the ability to interact with IRAK-1 this

argues that the wing region is dispensable for Pellino–IRAK binding. However, it does not exclude the possibility that the wing region may affect the affinity of the IRAK–Pellino interaction or mediate the interaction of Pellino proteins with other signalling molecules. It is interesting to note that viral Pellino can also bind to a kinase inactive form of IRAK-1. The latter would not be subjected to autophosphorylation and thus viral Pellino, via its FHA domain, likely recognises amino acid residues in IRAK-1 that are phosphorylated by upstream kinases such as IRAK-4.

Given that viral Pellino lacks a functional RING domain, these studies are consistent with the earlier findings that the RING domain of Pellino proteins is not required for IRAK-1 binding [18]. However, the RING domain of mammalian Pellinos is essential to promote polyubiquitination of IRAK-1 [15] and given its lack of a complete and functional RING domain, viral Pellino, proved, as expected, incapable of effecting any post-translational modification of IRAK-1. This is evidenced in the present study by virtue of the intense electrophoretic streaking of IRAK-1 when co-expressed with Pellino3S (Fig. 5A, last lane). On the contrary, the viral Pellino–IRAK-1 association leads to no such post-translational modification of IRAK-1 (see discrete IRAK bands in second panel of Fig 4A). As the precise functional consequences of Pellino-mediated IRAK-1 ubiquitination have not been elucidated and indeed may vary across the TLR family [30], it is not possible to say whether this divergence in activity between mammalian and viral Pellinos accounts for the inhibitory activity of the latter. It has, however, been suggested that Pellino-mediated IRAK-1 poly-ubiquitination may have a positive effect on signal transduction by inducing dissociation of IRAK/TRAF6/TAK-1/TAB-1 complexes or through promoting IRAK-NEMO interactions [14, 16]. In this light, viral Pellino may negatively influence flux through the pathway by competing for binding to IRAK-1 and antagonising the actions of mammalian Pellinos. Indeed, the present studies are consistent with a model where viral Pellino competes with mammalian Pellinos for binding to IRAK and in doing so inhibits poly-ubiquitination of IRAK-1 and subsequent downstream signalling. However, the expression of viral Pellino also leads to dramatic IRAK-1-induced depletion of Pellino3 and this provides a very novel mechanism by which a viral homolog can target its mammalian counterpart by promoting its degradation.

The targeting of IRAK-1 is unlikely to be the sole contributing mechanism to the inhibitory effects of viral Pellino on TLR signalling. Such a proposal is based on our demonstration that viral Pellino mutants, that fail to interact with IRAK-1, retain some inhibitory activity. Furthermore, our studies suggest that viral Pellino may potentially target TIR adaptor proteins such as Mal and MyD88, leading to their depletion. Such a targeted degradation of TIR adaptors, as an immunoevasive strategy, would not be without precedent given the recent report that Gram-negative bacteria belonging to the Brucella species encode a protein called TcpB that subverts innate immune signalling by targeting Mal for degradation [31]. The lack of a RING domain in viral Pellino argues against a direct mechanism by which it promotes polyubiquitination and degradation of Mal. In light of

the recent report that Pellino1 facilitates TRIF-dependent signalling [32], it is surprising to note that the Mal/MyD88 pathway is more sensitive than TRIF and TRAM to viral Pellino. However, the physiological roles of Pellino2 and Pellino3 remain to be fully elucidated and it will be interesting to explore the relative sensitivities of each of the mammalian Pellinos to viral Pellino.

Irrespective of the exact mechanism, the targeting of receptor proximal adaptor proteins by viral Pellino will lead to regulatory effects on a number of downstream signalling pathways. Indeed, the present studies show that viral Pellino can inhibit the p38 MAPK pathway as well as NF-κB. p38 MAPK co-ordinates inflammatory gene expression at numerous levels – regulating the activity of immunologically relevant transcription factors such as ATF-2 and CREB, activating pathways that extend the mRNA half-life of inflammatory mediators such as TNF [33] and dictating accessibility of a range of inflammatory response gene promoters to activated transcription factors by controlling histone phosphorylation status [34].

In conclusion, this study provides for the first time a detailed characterisation of a viral homolog of the Pellino family. In a potential immunoevasive strategy, viral Pellino targets its mammalian counterparts and receptor proximal signalling events in TLR pathways and further highlights the important emerging roles of Pellinos in innate immunity.

Materials and methods

Biological reagents and expression constructs

C-106 ligand was a gift from Nick Gay (Cambridge University, UK). The myc-tagged codon-optimised form of the viral Pellino gene was synthesised by Genscript Corporation (Piscataway, New Jersey, USA) and subcloned into the pCDNA3.1/Zeo mammalian expression vector (Invitrogen). Myc-tagged viral Pellino truncation mutants, lacking the most N-terminal 90 and 50 amino acids (ΔF1-myc and ΔF2-myc, respectively), and the point mutants of viral Pellino, (R33A and S47A, generated using the Quik Change Site-Directed Mutagenesis kit, Stratagene) were also cloned into pCDNA3.1. The myc-tagged form of the viral Pellino gene was sub-cloned into pAc5.1/V5 for expression in insect cells. Anti-IRAK-1 and anti-ubiquitin antibodies were from Santa Cruz Biotechnology. Monoclonal anti-myc antibody was from Cell Signalling Technology. Anti-Flag and anti-β-actin were from Sigma-Aldrich. Recombinant forms of ubiquitin, E1 and E2 (UbcH13/Uev1a) were from Boston Biochem. The His-tagged vector pRSET A was from Invitrogen. LPS was from Alexis Biochemicals. The generation of the construct encoding Pellino3S has been described previously [26]. Constructs encoding wild-type IRAK-1, IRAK-1 kinase-dead and TRAF6 were from Tularik (San Francisco, CA, USA). Constructs encoding MyD88, Mal and IKKβ were gifts from Luke O'Neill (Trinity College Dublin). pGL3-*Renilla* was a gift from Andrew Bowie (Trinity College Dublin).

The *drosomycin* promoter–reporter construct, the pACH110 vector containing the β-galactosidase gene under the control of the *Drosophila* actin promoter, and the pAc5.1/V5 *Drosophila* expression vector were all kind gifts from Jean-Luc Imler (Institut de Biologie Moleculaire et Cellulaire, Strasbourg, France).

Homology modeling

Two crystal structures of Pellino2, available in the Protein Data Bank (http://www.rcsb.org/pdb), PDB: 3EGA at 1.8 Å and 3EGB at 3.3 Å [18], were used as templates for comparative modelling. The former codes for residues 15–258 and the later codes for 15–276 of the Pellino2 sequence with a number of small gaps where residues could not be refined. Modeller 9v5 [21] was used to generate multiple models of viral Pellino modeled as an FHA domain using both Pellino2 templates and manually optimizing the alignment. The C-terminal region of the model was removed from Thr155 of viral Pellino as there was no template structure available for this region. A subsequent Modeller9v5 sequence identity score of 27.6% was achieved and models were shortlisted for subsequent analysis based on the Modeller objective function. The best model was minimised using MOE 2008 (http://www.chemcomp.com) in a 5 Å water sphere using the Amber99 force field.

Molecular dynamics

All molecular dynamics simulations were performed with Amber 10.0 [35] using a time step of 1 fs and the Amber force field. Periodic boundary conditions were applied in all three dimensions with the Particle Mesh Ewald (PME) method being used to treat the long-range electrostatic interactions. Non-bonded interactions were calculated for one to four interactions and higher using a cutoff radius of 9 Å. The protein was placed in a TIP3P water box with 12 Å to the box edge. Counter ions (Cl$^-$) were added to ensure a charge neutral cell, by replacing solvent molecules at sites of high electrostatic potential. Each simulation cell, prior to MD, was optimised to remove bad contacts by performing 250 steps of steepest descent followed by 750 steps of conjugate gradient energy minimisation. The simulation cell was heated gradually to 300 K over 10 ps with equilibration performed using backbone restraints for 10 ps at each of 15, 10 and 5 kcal/mol followed by 960 ps without restraints. Root mean square deviations were calculated for the backbone heavy atoms after fitting the Cα carbons to the initial structure as a reference.

Generation of recombinant viral Pellino and in vitro ubiquitination assay

Myc-tagged viral Pellino and Pellino3S were cloned into the vector pRSET A-His, expressed in *Escherichia coli* (BL21 cells) and

purified using the His-bind purification kit (Qiagen). For the in vitro ubiquitination assay, recombinant Pellino protein (1 μg) was incubated with ubiquitin (1 μg), E1 (50 ng), UbcH13/Uev1a (400 ng) and protease inhibitor mix (EDTA free) in 5 mM Tris-HCl, pH 7.5, containing $MgCl_2$ (2 mM), ATP (2 mM) and NaCl (100 mM). Reactions were incubated at 37°C for 2 h and terminated by addition of SDS-PAGE sample buffer. Samples were then resolved by SDS-PAGE and analysed by immunoblotting using an anti-ubiquitin antibody (Santa Cruz).

Cell culture

Drosophila Schneider 2 (S2) cells were cultured in Schneider's Insect Medium supplemented with 10% v/v fetal bovine serum, penicillin G (100 μg/mL) and streptomycin (100 μg/mL). Cells were maintained at 25°C without CO_2 buffering. C-106 stimulation was performed on cells in serum-containing medium at 25°C. HEK293T cells and HEK 293-TLR4 cells (gift from Douglas Golenbock) and U373 cells were cultured in DMEM supplemented with 10% v/v fetal bovine serum, penicillin G (100 μg/mL) and streptomycin (100 μg/mL). G418 (0.5 mg/mL) was used as a selective agent for the stably transfected 293-TLR4 cells. LPS stimulation was performed on cells in serum-containing medium at 37°C.

Transfection of HEK 293 cells

Cells were seeded at 1.8×10^5 and 2×10^5/mL, respectively, in 96-well plates (200 μL/well) and 6-well plates (3 mL/well) and grown for 24 h to approximately 80% confluency. Cells were transfected using Lipofectamine (Invitrogen), with each well in a 6-well and 96-well plate being transfected with 4 μg and 230 ng total DNA, respectively. For 96-well plate transfections, lysates were generated using Reporter Lysis Buffer (Sigma). Firefly activity and *Renilla* luciferase activities were assayed using luciferase substrate (Promega) and coelenterazine (0.1 μg/mL in PBS), respectively.

Transfection of Drosophila S2 cells

Cells were seeded at 2×10^6/mL in 12-well plates and grown for 24 h. Transfection was then performed using the Calcium Phosphate Transfection kit (Invitrogen) according to the manufacturer's instructions. For each well, a total of 1 μg DNA was used. In total, 24 h post-transfection cells were washed twice in serum-free Schneider's Medium, re-seeded in fresh medium and stimulated overnight with or without C-106 ligand. Lysates were generated with Reporter Lysis Buffer (Promega) and assayed for firefly luciferase activity. β-Galactosidase activity was assayed by incubating cell lysate with *o*-nitrophenyl-β-galactoside (1 mg/mL) at 37°C for 15 min before reading absorbance at 420 nm.

Immunoprecipitation and Western blot analysis

Briefly, 24 h post-transfection, cells were lysed in 50 mM Tris-HCl (pH 7.5) containing 150 mM NaCl, 0.5% v/v Igepal, 50 mM NaF, 1 mM Na_3VO_4, 1 mM dithiothreitol, 1 mM phenylmethylsulfonyl fluoride, protease inhibitor mixture (25 μg/mL leupeptin, 25 μg/mL aprotinin, 1 mM benzamidine and 10 μg/mL trypsin inhibitor). An aliquot (50 μL) of supernatant was retained for Western blot analysis and the remainder was subjected to immunoprecipitation.

Lysates were precleared by addition of IgG antibody (1 μg) and re-suspended Protein A/G-agarose (10 μL). IP with the appropriate antibody (2 μg per sample) was overnight at 4°C. Antibody–protein complexes were pelleted after addition of Protein A/G-agarose (35 μL). Samples were boiled in reducing sample buffer and immunoprecipitates subjected to SDS-PAGE and Western blot analysis.

CHOP reporter system

The PathDetect CHOP trans-reporting system (Stratgene, La Jolla, CA, USA) was used, according to the manufacturer's recommendations, to measure activation of the p38 MAPK pathway. Briefly, HEK 293-TLR4 (1.8×10^5 cells/well) were seeded into 96-well plates and grown for 24 h. Cells were then transfected, using Lipofectamine 2000, with the GAL4-CHOP-regulated firefly luciferase reporter plasmid pFR-Luc (60 ng), the trans-activator plasmid pFA-CHOP (activation domain of CHOP fused with the yeast Gal4 DNA binding domain) (1 ng), constitutively expressed *Renilla*-luciferase reporter construct (pGL3-*Renilla*, 20 ng) and with or without Pellino3S or viral Pellino expression constructs. Luciferase activities were analysed as described above.

Microscopic analysis of subcellular localisation of MAPKAP kinase 2-Ds Red [26]

HEK 293T cells (1.6×10^5/well) were seeded into 4-well Lab-Tek chamber slides (Nunc A/S, DK-4000, Denmark) and grown for 24 h. Cells were then transfected, using Lipofectamine, with MAPKAP kinase 2-Ds Red (400 ng) in the presence or absence of Pellino3- or viral Pellino-GFP (400 ng). Cells were fixed in 4% paraformaldehyde for 15 min, washed three times with PBS and mounted with Slowfade antifade reagent [DAPI containing medium (1.5 μg/mL)] (Molecular Probes, USA). Confocal images were captured using the ×63 objective (oil immersion) on the UV Zeiss 510 Meta System laser-scanning microscope equipped with the appropriate filter sets and analysed using the LSM 5 browser imaging software.

Lentiviral transduction of THP-1 cells

The myc-tagged form of the viral Pellino gene was sub-cloned into the lentiviral vector pLV-CMV-GFP. Lentiviral particles

encoding vPellino were generated by transfecting HEK293T cells with a viral packaging plasmid pPTK (900 ng), a viral envelope plasmid pMDG (100 ng) and pLV-CMV-GFP encoding vPellino (1 µg) or an empty pLV-CMV-GFP vector using Lipofectamine 2000. In total, 24 h post-transfection, the medium was replaced with DMEM supplemented with 30% v/v fetal bovine serum. A total of 24, 48 and 72 h later, medium containing virus was harvested and stored at −20°C with DMEM, supplemented with 30% FBS, added to cells after each harvesting. The pooled virus stocks were titred.

THP-1 cells were plated at 2×10^5 cells/mL in 96-well suspension plates (100 µL/well), supplemented with hexadimethrine bromide (8 µg/mL). On the day of seeding, cells were transduced with lentivirus. The media was removed 24 post-infection and replaced with fresh RPMI medium. The medium was replaced for further 2 days before cells were used in experiments. Mammalian U373 and insect S2 cell lines were transduced with viral particles in the same way.

Cytokine immunoassays

Conditioned media from cells were assayed for the levels of IL-8 and TNF by sandwich ELISA [DuoSet kit (R&D Systems)] according to the manufacturer's instructions.

Conflict of interest: The authors declare no financial or commercial conflict of interest.

References

1 Takeda, K. and Akira, S., Toll-like receptors in innate immunity. *Int. Immunol.* 2005. **17**: 1–14.

2 Lemaitre, B., The road to Toll. *Nat. Rev. Immunol.* 2004. **4**: 521–527.

3 Medzhitov, R., Preston-Hurlburt, P., Kopp, E., Stadlen, A., Chen, C., Ghosh, S. and Janeway, C. A., Jr., MyD88 is an adaptor protein in the hToll/IL-1 receptor family signaling pathways. *Mol. Cell* 1998. **2**: 253–258.

4 Horng, T., Barton, G. M., Flavell, R. A. and Medzhitov, R., The adaptor molecule TIRAP provides signalling specificity for Toll-like receptors. *Nature* 2002. **420**: 329–333.

5 Li, S., Strelow, A., Fontana, E. J. and Wesche, H., IRAK-4: a novel member of the IRAK family with the properties of an IRAK-kinase. *Proc. Natl. Acad. Sci. USA* 2002. **99**: 5567–5572.

6 Xia, Z. P., Sun, L., Chen, X., Pineda, G., Jiang, X., Adhikari, A., Zeng, W. and Chen, Z. J., Direct activation of protein kinases by unanchored polyubiquitin chains. *Nature* 2009. **461**: 114–119.

7 Deng, L., Wang, C., Spencer, E., Yang, L., Braun, A., You, J., Slaughter, C. et al., Activation of the IkappaB kinase complex by TRAF6 requires a dimeric ubiquitin-conjugating enzyme complex and a unique polyubiquitin chain. *Cell* 2000. **103**: 351–361.

8 Wang, C., Deng, L., Hong, M., Akkaraju, G. R., Inoue, J. and Chen, Z. J., TAK1 is a ubiquitin-dependent kinase of MKK and IKK. *Nature* 2001. **412**: 346–351.

9 Karin, M. and Ben-Neriah, Y., Phosphorylation meets ubiquitination: the control of NF-[kappa]B activity. *Annu. Rev. Immunol.* 2000. **18**: 621–663.

10 Schauvliege, R., Janssens, S. and Beyaert, R., Pellino proteins: novel players in TLR and IL-1R signalling. *J. Cell. Mol. Med.* 2007. **11**: 453–461.

11 Moynagh, P. N., The Pellino family: IRAK E3 ligases with emerging roles in innate immune signalling. *Trends Immunol.* 2009. **30**: 33–42.

12 Grosshans, J., Schnorrer, F. and Nusslein-Volhard, C., Oligomerisation of Tube and Pelle leads to nuclear localisation of dorsal. *Mech. Dev.* 1999. **81**: 127–138.

13 Haghayeghi, A., Sarac, A., Czerniecki, S., Grosshans, J. and Schock, F., Pellino enhances innate immunity in Drosophila. *Mech. Dev.* 2010. **127**: 301–307.

14 Schauvliege, R., Janssens, S. and Beyaert, R., Pellino proteins are more than scaffold proteins in TLR/IL-1R signalling: a role as novel RING E3-ubiquitin-ligases. *FEBS Lett.* 2006. **580**: 4697–4702.

15 Butler, M. P., Hanly, J. A. and Moynagh, P. N., Kinase-active interleukin-1 receptor-associated kinases promote polyubiquitination and degradation of the Pellino family: direct evidence for PELLINO proteins being ubiquitin-protein isopeptide ligases. *J. Biol. Chem.* 2007. **282**: 29729–29737.

16 Ordureau, A., Smith, H., Windheim, M., Peggie, M., Carrick, E., Morrice, N. and Cohen, P., The IRAK-catalysed activation of the E3 ligase function of Pellino isoforms induces the Lys63-linked polyubiquitination of IRAK1. *Biochem. J.* 2008. **409**: 43–52.

17 Smith, H., Peggie, M., Campbell, D. G., Vandermoere, F., Carrick, E. and Cohen, P., Identification of the phosphorylation sites on the E3 ubiquitin ligase Pellino that are critical for activation by IRAK1 and IRAK4. *Proc. Natl. Acad. Sci. USA* 2009. **106**: 4584–4590.

18 Lin, C. C., Huoh, Y. S., Schmitz, K. R., Jensen, L. E. and Ferguson, K. M., Pellino proteins contain a cryptic FHA domain that mediates interaction with phosphorylated IRAK1. *Structure* 2008. **16**: 1806–1816.

19 Afonso, C. L., Tulman, E. R., Lu, Z., Oma, E., Kutish, G. F. and Rock, D. L., The genome of *Melanoplus sanguinipes* entomopoxvirus. *J. Virol.* 1999. **73**: 533–552.

20 Rich, T., Allen, R. L., Lucas, A. M., Stewart, A. and Trowsdale, J., Pellino-related sequences from *Caenorhabditis elegans* and *Homo sapiens*. *Immunogenetics* 2000. **52**: 145–149.

21 Sali, A. and Blundell, T. L., Comparative protein modelling by satisfaction of spatial restraints. *J. Mol. Biol.* 1993. **234**: 779–815.

22 **Laskowski, R. A., Rullmannn, J. A., MacArthur, M. W., Kaptein, R. and Thornton, J. M.,** AQUA and PROCHECK-NMR: programs for checking the quality of protein structures solved by NMR. *J. Biomol. NMR* 1996. **8**: 477–486.

23 **Morris, A. L., MacArthur, M. W., Hutchinson, E. G. and Thornton, J. M.,** Stereochemical quality of protein structure coordinates. *Proteins* 1992. **12**: 345–364.

24 **Barrett, J. W., Sun, Y., Nazarian, S. H., Belsito, T. A., Brunetti, C. R. and McFadden, G.,** Optimization of codon usage of poxvirus genes allows for improved transient expression in mammalian cells. *Virus Genes* 2006. **33**: 15–26.

25 **Strelow, A., Kollewe, C. and Wesche, H.,** Characterization of Pellino2, a substrate of IRAK1 and IRAK4. *FEBS Lett.* 2003. **547**: 157–161.

26 **Butler, M. P., Hanly, J. A. and Moynagh, P. N.,** Pellino3 is a novel upstream regulator of p38 MAPK and activates CREB in a p38-dependent manner. *J. Biol. Chem.* 2005. **280**: 27759–27768.

27 **Jensen, L. E. and Whitehead, A. S.,** Pellino2 activates the mitogen activated protein kinase pathway. *FEBS Lett.* 2003. **545**: 199–202.

28 **Harte, M. T., Haga, I. R., Maloney, G., Gray, P., Reading, P. C., Bartlett, N. W., Smith, G. L. et al.,** The poxvirus protein A52R targets Toll-like receptor signaling complexes to suppress host defense. *J. Exp. Med.* 2003. **197**: 343–351.

29 **Mack, C., Sickmann, A., Lembo, D. and Brune, W.,** Inhibition of proinflammatory and innate immune signaling pathways by a cytomegalovirus RIP1-interacting protein. *Proc. Natl. Acad. Sci. USA* 2008. **105**: 3094–3099.

30 **Qin, J., Yao, J., Cui, G., Xiao, H., Kim, T. W., Fraczek, J., Wightman, P. et al.,** TLR8-mediated NF-kappaB and JNK activation are TAK1-independent and MEKK3-dependent. *J. Biol. Chem.* 2006. **281**: 21013–21021.

31 **Sengupta, D., Koblansky, A., Gaines, J., Brown, T., West, A. P., Zhang, D., Nishikawa, T. et al.,** Subversion of innate immune responses by Brucella through the targeted degradation of the TLR signaling adapter, MAL. *J. Immunol.* 2010. **184**: 956–964.

32 **Chang, M., Jin, W. and Sun, S. C.,** Peli1 facilitates TRIF-dependent Toll-like receptor signaling and proinflammatory cytokine production. *Nat. Immunol.* 2009. **10**: 1089–1095.

33 **Wang, S. W., Pawlowski, J., Wathen, S. T., Kinney, S. D., Lichenstein, H. S. and Manthey, C. L.,** Cytokine mRNA decay is accelerated by an inhibitor of p38-mitogen-activated protein kinase. *Inflamm. Res.* 1999. **48**: 533–538.

34 **Saccani, S., Pantano, S. and Natoli, G.,** p38-Dependent marking of inflammatory genes for increased NF-kappa B recruitment. *Nat. Immunol.* 2002. **3**: 69–75.

35 **Case, D. A., Darden, T. A., Cheatham, I. T. E., Simmerling, C. L., Wang, J., Duke, R. E., Luo, R. et al.,** *Amber 10*, University of California, San Francisco, CA 2008.